International Journal of Technology 11(2) 422-435 (2020)
Received March 2018 / Revised March 2020 / Accepted April 2020

International Journal of Technology

http://ijtech.eng.ui.ac.id

Synthesis of Nano-silica from Boiler Ash in the Sugar Cane Industry using the Precipitation Method

Nastiti Siswi Indrasti[1*], Andes Ismayana[1], Akhiruddin Maddu[2], Sasongko Setyo Utomo[1]

[1]*Department of Agroindustrial Technology, Institut Pertanian Bogor (IPB) University, Jl. Raya Dramaga, Bogor 16680, Indonesia*
[2]*Department of Physics, Institut Pertanian Bogor (IPB) University, Jl. Raya Dramaga, Bogor 16680, Indonesia*

Abstract. Boiler ash is a second layer by-product of the combustion of fuel, usually an agro-waste, in any industry. In the sugarcane industry, boiler ash is obtained from the combustion of bagasse. The boiler ash of the sugarcane industry contains 49.69% silica, which can be transformed into nano-silica using the precipitation method, which is easier and cheaper than other methods. Precipitation pH and aging time are the main factors that influence nano-silica's characteristics. The objectives of this research were to determine the effect of various precipitation pH levels and aging times on the characteristics of nano-silica and to identify the potential applications of nano-silica based on these characteristics. An increase in precipitation pH affected the number of the crystal phase and the intensity of the diffraction peaks. An increase in aging time also affected the intensity of the diffraction peaks and the number of crystal phases. The degree of crystallinity varied from 66.40% to 93.53%, the crystal size ranged from 37.77 nm to 56.87 nm, the particle size ranged from 214.04 nm to 698.24 nm, and the polydispersity index (PDI) ranged from 0.21 to 0.83. The nano-silica in this research had polygonal morphology. Increases in precipitation pH and aging time increased the number of siloxane groups, creating nano-silica dominated by a crystalline form with three crystal phases: tridymite, quartz, and cristobalite. Nano-silica have various potential applications based on their characteristics, including as filler for membranes, composite resin, rubber airbags, and supplementary cementitious material.

Keywords: Boiler ash; Characteristics; Nano-silica; Precipitation; Silica

1. Introduction

Boiler ash is a second layer by-product from the combustion of fuel, usually an agro-waste, in any industry. Sugar-cane bagasse ash (SCBA) is a by-product of bagasse combustion in the sugar cane industry. SCBA is mostly fine particulate silica with minor alumino-silicates and is produced when bagasse is burned for the co-generation of heat and electricity at a sugar mill (Arif et al., 2017). Silica also can be extracted from various sources, such as rice husk ash (Dhaneswara et al., 2020), fly ash tiles (Yadav et al., 2020), bamboo leaves (Dileep and Narayanankutty, 2020), coal fly ash (Lee et al., 2017), corn cob ash (Okoronkwo et al., 2013), mud, the fly ash of the palm oil industry, and natural sand (Munasir et al., 2013).

*Corresponding author's email: nastiti.indrasti@gmail.com, Tel.: +62 251 8627830; Fax.: +62 251 8627830
doi: 10.14716/ijtech.v11i2.1741

Boiler ash from the sugar cane industry is 49.69% silica, while furnace ash is 78.75% silica (Ismayana et al., 2017). The synthesis of silica from boiler ash not only produces valuable silica but also reduces pollution problems caused by the uncontrolled combustion of the ash (Dhaneswara et al., 2020). The development of nanoscale particles (nanoparticles) has recently become the object of attention for researchers due to their unique properties, such as their very small size, high surface area, and surface activity (Dileep and Narayanankutty, 2020). One of the nanoparticles focused upon in current research is nano-silica. In some applications, nano-silica has been used as an adsorbent, catalyst support material, a semiconductor, thermal insulation, and a ceramic filler (Adam et al., 2011).

The high content of silica-induced boiler ash is transformed into nano-silica, and its characteristics and utilization are more extensive because of the larger surface area. There are several methods for synthesizing nano-silica, such as microemulsion, thermal decomposition, the sol-gel method (Okoronkwo et al., 2013), ultrasonication (Ismayana et al., 2017), and precipitation (Mahdavi et al., 2013).

The precipitation method has many advantages; it is easy and cheap, operates at a low process temperature, uses a low amount of energy, and produces nano-silica of high purity and good quality (Mahdavi et al., 2013). It is also safe and environmentally friendly (Shahmiri et al., 2013). The main factors that influence the nano-silica produced through the precipitation method are precipitation pH and aging time. Various combinations of precipitation pH and aging time result in nano-silica with different characteristics. According to Singh et al. (2012), an increase in pH increases crystal size. Allaedini and Muhammad (2013) found that the crystal size of a nanoparticle is closely linked to the diffraction pattern, the crystalline phase, the particle size, and the degree of crystallinity. In addition, a longer aging time causes a higher degree of crystallinity (Jalilpour and Fathalilou, 2012).

The objectives of this research were to synthesize nano-silica from the boiler ash in the sugarcane industry using the precipitation method and to determine the effect of pH precipitation and aging time on the characteristics of the nano-silica. This research also aimed to identify potential applications based on the characteristics of the nano-silica produced.

2. Methods

2.1. Materials and Equipment

Boiler ash was obtained from the Gunung Madu sugarcane plantation in Lampung, Indonesia. Ammonium hydroxide (pa grade) and hydrochloric acid (pa grade) were obtained from Merck. The other materials used were Whatman 42 filter paper and distilled water. The equipment used in this research consisted of a furnace, reflux equipment, a magnetic stirrer, and pH meters. The analysis equipment included a particle size analyzer (PSA) (Vasco), an x-ray fluorescence (XRF) OPTX ARL-2050 analyzer, an x-ray diffraction (XRD) (GBC Emma), and a Fourier transform infrared (FTIR) Tensor 37 spectrometer (Bruker Optics).

2.2. Preparation of the Boiler Ash

The boiler ash was washed using distilled water. Then, it was dried in a blower for five hours, filtered using a coarse sieve, and finally burned at 700°C for six hours using a furnace (Thuadaij and Nuntiya, 2008).

2.3. Silica Extraction from the Furnace Ash

Ten grams of furnace ash were extracted with 80 ml of NaOH 2.5 N for three hours. The solution was filtered, and the residue was washed using 20 ml of boiling distilled water. The filtrate was cooled at room temperature. The filtrate was added with H_2SO_4 5 N until it reached pH 2 and with NH_4OH 2.5 N until it reached pH 8.5. The solution was then left at

room temperature for 3.5 hours for aging. Next, the solution was dried at 105°C for 12 hours (Thuadaij and Nuntiya, 2008; Setiawan et al., 2015; Ismayana et al., 2017).

2.4. Synthesis of the Nano-silica

The silica was hydrolyzed using 3 N HCl for six hours. Next, the solution was filtered and washed with distilled water to remove excess acid to achieve a neutral pH. The neutral residue dissolved in 2.5 N NaOH using a magnetic stirrer for eight hours. A 5 N H_2SO_4 solution was added until the pH reached 7, 8, 9, or 10. The solution was allowed to age at room temperature for three and six hours each. Then, it was dried at a temperature of 105°C for 12 hours in the oven (Setiawan et al., 2015; Ismayana et al., 2017).

2.5. Characterization of the Nano-silica

The compound and the element of the boiler and furnace ash were analyzed with XRF ARL OPTX-2050. The particle size and the particle size distribution were observed with PSA. A total of 0.02 g nano-silica powder was dispersed in distilled water and rotated with a magnetic stirrer for 15 minutes. The nano-silica particles were scanned using PSA for 2-5 minutes.

The crystal size, degree of crystallinity, and crystalline phase were observed using XRD GBC Emma operated at 35 kV and 25 mA. The calculation of the degree of crystallinity was run using PowderX software by dividing the crystal area to the total area, while the crystal size was determined using the Scherrer Equation 1.

$$D = \frac{k\lambda}{\beta\cos\theta} \quad (1)$$

where k is the Scherrer constant (0.9), λ is the wavelength of Cu-Kα (0.154056 nm), β is full width at half maximum (FWHM), and θ is the phase angle.

The diffraction pattern and the crystal phase were identified through matching with a powder diffraction file (PDF) card using Match! 2 software. The chemical composition was analyzed using energy dispersion x-ray (EDX) spectroscopy, and the formation of functional groups on the nano-silica was characterized using FTIR Tensor 37. The physical morphology of the synthesized nano-silica was identified using scanning electron microscopy (SEM).

3. Results and Discussion

3.1. Boiler Ash and Furnace Ash

The content of the silica from the boiler ash and the furnace ash was 49.69% and 78.75%, respectively. The higher silica content in the furnace ash occurred due to the process of amount normalization. Normalization increased the percentage of silica in the furnace ash because of the declining amount of other compounds as a result of the ashing process at 700°C. P_2O_5, Na_2O, and SO_3, have melting points of 44.19°C, 97.8°C, and 115.2°C, respectively (Bauccio, 1993). Al_2O_3, K_2O, CaO, and MgO have melting points of 660.45°C, 350°C, 840°C, and 649°C, respectively (Bauccio, 1993). Fe_2O_3 and silica (SiO_2) have melting points of 1535°C and 1414°C, respectively (Bauccio, 1993). The high melting points of Fe_2O_3 and SiO_2 increased their content. Table 1 shows the compounds in the boiler ash and the furnace ash.

3.2. Characteristics of Nano-silica

3.2.1. Diffraction patterns and crystal phase

The analysis of the diffraction pattern and the crystal phase using XRD indicated that an increase in the precipitation pH at three hours of aging time, as well as at six hours,

increased the number and intensity of the diffraction peaks. The condensation reaction of the nanoparticle compounds occurred as the pH value increased (Jarvenin, 2013).

Table 1 Compound content of the boiler ash and the furnace ash

No.	Compound	Boiler Ash (%)	Furnace Ash (%)
1	SiO_2	49.69	78.75
2	Al_2O_2	11.24	10.36
3	K_2O	8.76	1.80
4	P_2O_5	8.14	0.00
5	Na_2O	7.00	0.00
6	CaO	4.95	0.89
7	MgO	3.59	1.06
8	Fe_2O_3	3.23	5.37
9	SO_3	1.63	0.00
10	TiO_2	0.79	0.62

A higher precipitation pH resulted in a lower nucleation rate rather than the growth of the primary particles. The primary particle growth was caused new crystal formation from the existing crystal nucleus. The new crystals caused an increase in the number of diffraction peaks and crystal phases. Moreover, the increasing number of diffraction peaks and the forming of new crystals increased the intensity of the diffraction peaks due to the increasing number of crystal phases in a 2θ value. Figure 1 shows the diffractogram of the nano-silica in three phases; quartz, cristobalite, and tridymite.

The analysis of the diffraction pattern and the crystal phase indicated that increasing the aging time increased the diffraction phase intensity. The aging process allows for the termination and reprecipitation of the silica monomer into a stronger and stiffer gel structure. In other words, during the aging process, the strength and stiffness of the gel increased (Nidhin et al., 2008). Therefore, the intensity of the diffraction peaks increased as the aging time increased due to the strengthening of the crystal structure. Based on the crystal phase analysis, it was evident that the nano-silica was composed of the multiphase characteristics of a crystal. In fact, three kinds of crystal phases (quartz, cristobalite, and tridymite) were identified in each condition, as shown in Figure 1.

3.2.2. Degree of crystallinity

The degree of crystallinity was closely linked to the pattern of diffraction and the crystal phase of the nano-silica. The degree of crystallinity varied from 66.40% to 93.53%. The increase in precipitation pH increased the degree of crystallinity, as shown in Table 2. Increase in the degree of crystallinity related to the new diffraction peak due to the growth of primary particles when high precipitation pH was applied. Increasing the number of diffraction peaks increased the number of the crystal phase, which increased the degree of crystallinity (Jalilpour and Fathalilou 2012). Increasing the intensity of the diffraction peaks also increased the degree of crystallinity. The increase in intensity was due to the increasing number of crystal phases at 2θ values.

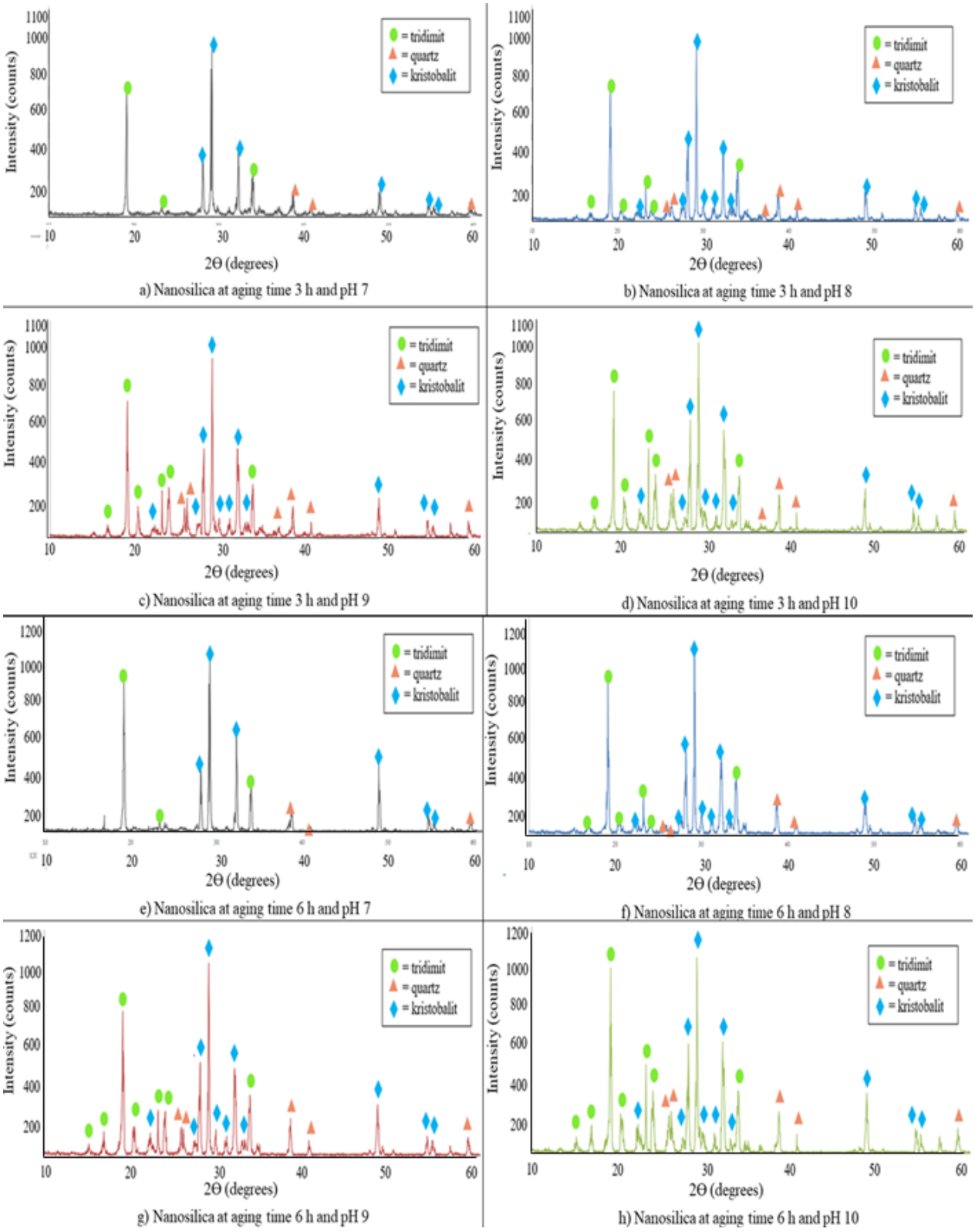

Figure 1 The diffractogram and the crystal phases of the nano-silica

Aging time also influenced the strength of the crystal structure. A longer aging time improved the strong structure of the crystal planes, and a strong crystal plane structure increased the intensity of the diffraction peaks. The high intensity of the diffraction peaks,

in turn, increased the degree of crystallinity. Table 2 shows the degree of crystallinity of the nano-silica at each condition.

Table 2 The degree of crystallinity, crystal size, particle size, and PDI of the nano-silica

Aging time (hours)	pH	Degree of crystallinity (%)	Average crystal size (nm)	Average particle size (nm)	PDI
3	7	66.39	37.77	214.04	0.21
	8	83.28	43.99	243.69	0.32
	9	86.50	47.02	345.89	0.35
	10	89.65	52.05	529.14	0.76
6	7	82.38	45.65	331.95	0.22
	8	86.08	51.86	338.69	0.42
	9	92.79	53.85	411.05	0.55
	10	93.53	56.87	698.24	0.83

3.2.3. Crystal size, particle size, and particle size distribution

An increase in the precipitation pH increased the average crystal size. This phenomenon relates to the process of primary particle growth when a high pH was applied. Primary particle growth produced a large crystal size as a result of the merger (aggregation) of the core crystal and other crystal nuclei. The condensation reaction of nanoparticle compounds occurred when an increased pH was applied and resulted in the growth of primary particles and larger-than- average crystal size (Jarvenin, 2013).

The high precipitation pH caused the primary particles to aggregate with other primary particles to form secondary particles, producing larger crystal and particle sizes (Happy et al., 2007). Increased precipitation pH reduced the electrostatic barrier around the primary particles and caused the agglomeration. The large crystal size directly affected the size of the produced particles.

The particle size was the result of the agglomeration process of the primary particles, meaning that each particle consisted of more than one crystal. The average crystal size, average particle size, and PDI of the nano-silica are shown in Table 2. According to Namazi et al. (2012), nanoparticles are the resolution of dispersed particles or solid particles with sizes on a scale from 10 nm to 1000 nm. As such, the nano-silicas produced in this research included the nanoscale. Moreover, a particle size over 100 nm produced some scattered light and decreased transparency (Ha et al., 2019).

Increased aging time caused the agglomeration process of the primary particle, which, in turn, caused an increase in the average crystal and particle sizes. Small particles in an aqueous suspension tent joined together and built larger aggregates (Jarvenin, 2013). Figure 2 shows the particle size distribution of the nano-silica.

The polydispersity index (PDI) is a parameter that describes the particle size distribution of nanoparticles. A PDI value of 0.01 indicates monodisperse nanoparticles, while a PDI value of 0.7 is considered within the tolerance limits of nanoparticles that can be used as supporting material in various applications. Nanoparticles with a very broad size distribution will have PDI values greater than 0.7 (Nidhin et al., 2008). A broad particle range impacts the PDI value, and a high PDI value indicates that the nano-silica sample was not uniform.

Figure 2a shows the particle size distribution curve when the aging time was three hours, while Figure 2b shows the size distribution curve at six hours of aging time. As pH increases, the PDI value increases. An increasing PDI value causes the size distribution

curve to widen due to the unstable primary particle growth process and the agglomeration process as the precipitation pH increases.

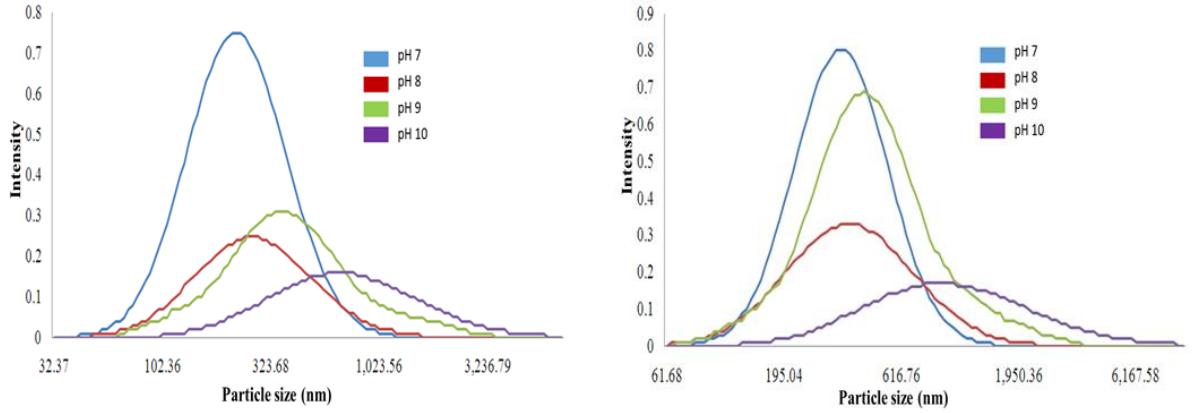

(a) (b)

Figure 2 Particle size distribution of the nano-silica at: (a) 3 h aging time; and (b) 6 h aging time

The processes of primary particle growth and agglomeration create the size uniformity of nano-silica. This is supported by the results of the analysis of the diffraction pattern parameters, the average size of the crystals, and the average size of the particles. The diffraction pattern when the pH precipitation is high leads to the emergence of new crystals due to the growth of the primary particles. In addition to increasing the size of the crystals and the particles, the process of agglomeration and the growth of primary particles makes the resulting size non-uniform. This non-uniformity is evidenced by the widening of the nano-silica particle size distribution curve.

3.2.4. Fourier transform infrared (FTIR) spectra

FTIR analysis can show the functional groups in a sample of nano-silica. The absorption band appears at a certain wave number, indicating the identity of certain functional groups in several samples. In addition, the intensity of a certain functional group shows the number of the functional group in a sample. Figure 3 shows the FTIR spectra of the nano-silica at pH 7 and pH 10 and aging times of three hours and six hours.

Figures 3a and 3c show the FTIR spectra at an aging time of three hours. The absorption bands of the two samples have similarities but different intensities. In the pH 10 treatment, the absorption bands formed at 3398.39, 1626.15, 1060.64, 986.45, and 794.45. According to Sriyanti et al. (2005), the absorption band at wave numbers around 3400 cm^{-1} shows the vibration of the -OH (hydroxyl) group of the silanol group (Si-OH). The absorption band at the wave number around 1600 cm^{-1} showed the bend-OH vibration of the silanol group. The absorption band at the wave number around 1100 cm^{-1} showed the stretch vibration of the siloxane group (Si-O-Si). Meanwhile, the absorption bands at wave numbers around 900 cm^{-1} and 700 cm^{-1} showed the stretching vibrations of Si-OH (silanol) and Si-O-Si (siloxane), respectively.

In the pH 7 treatment, the FTIR spectra did not differ much from that of the pH 10 treatment. Absorption bands appeared at wave numbers 3423.56, 1603.34, 1104.54, 990.87, and 786.45. The absorption band showed -OH (hydroxyl) vibrations from silanol (Si-OH), bend -OH vibrations from water, siloxane group stretching vibrations (Si-O-Si), stretching vibrations from silanol (Si-OH), and stretch vibrations from siloxane (Si-O-Si) in a row.

In the absorption band wave of 3400 cm^{-1} at pH 7 and aging times of three hours and

six hours, the intensity was higher than in the absorption bands at pH 10 with aging times of three hours and six hours, indicating that the silanol groups at pH 10 were lower than the silanol groups at pH 7.

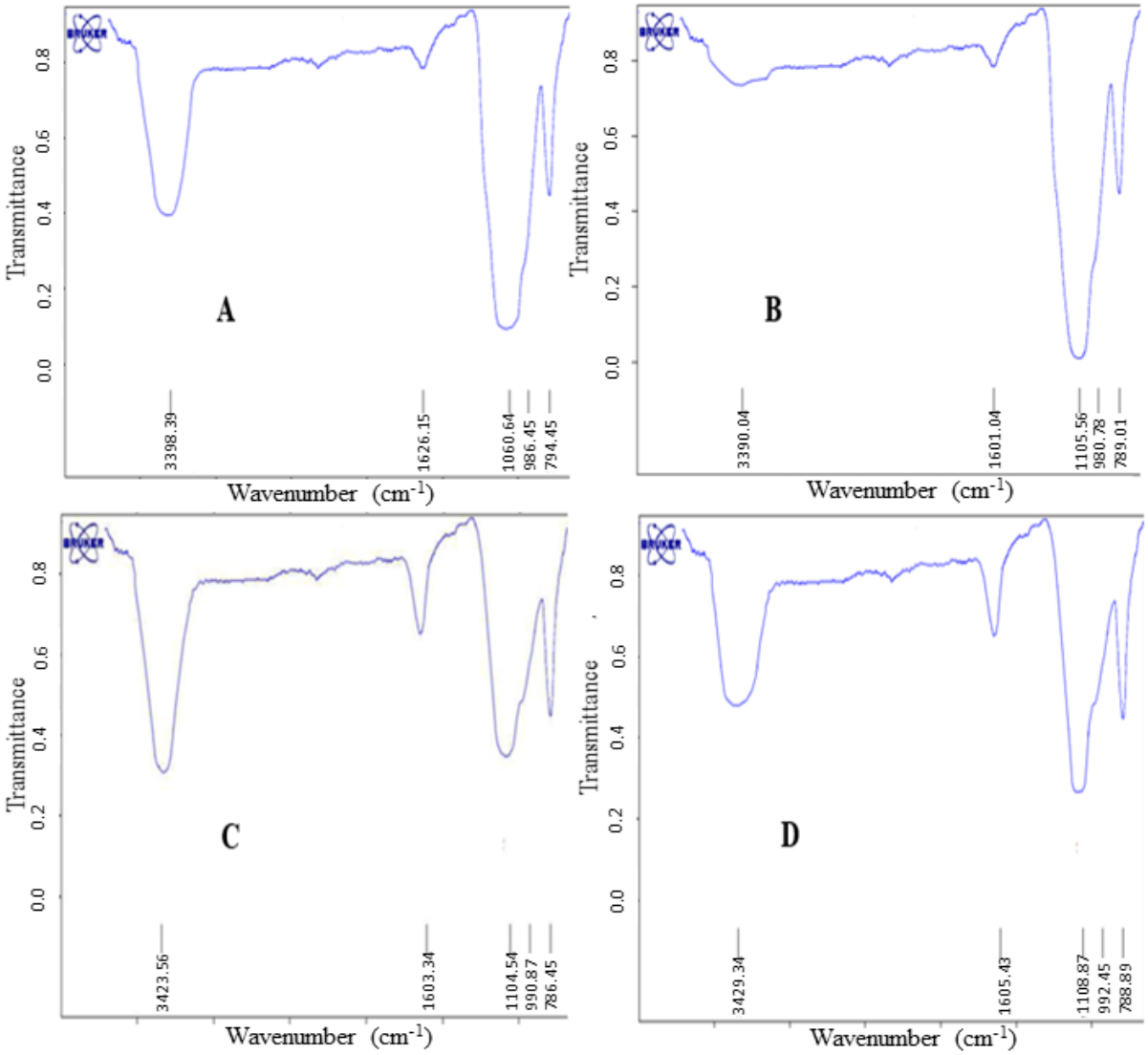

Figure 3 FTIR spectra of the nano-silica at: (a) pH 10 with an aging time of 3 h; (b) pH 10 with an aging time of 6 h; (c) pH 7 with an aging time of 3 h; and (d) pH 7 with an aging time of 6 h

In the absorption band wave of 1100 cm^{-1} at pH 7, the intensity was lower than in the absorption band of pH 10, indicating that the siloxane groups at pH 10 were higher than at pH 7. At pH 10, the siloxane groups increased and the silanol groups decreased, indicating a condensation reaction of the silica compound at pH 10. This condensation reaction occurred between one silanol group and another silanol group and formed siloxane groups. The condensation reaction was caused by the agglomeration process of the silica compounds. The intensity of the silanol groups at pH 7 was higher than at pH 10 because of the low agglomeration process at pH 7. This phenomenon was proven by the fact that the intensity of absorption band of the siloxane groups at pH 7 was lower than at pH 10.

Figures 3b and 3d showed the FTIR spectra at an aging time of six hours. The absorption bands of the two samples had similarities to the absorption bands of the samples when the aging time was three hours. In the pH 10 and pH 7 treatments, absorption bands were formed at about 3400, 1600, 1100, 900 and 700 cm^{-1} wave numbers. These absorption

bands indicated the vibration of the -OH (hydroxyl) group of the silanol (Si-OH) group, the bend -OH vibration of the group silanol, stretching vibrations of the siloxane group (Si-O-Si), stretching vibrations of Si-OH (silanol), and Si-O-Si (siloxane), respectively.

3.2.5. Morphology of the nano-silica

The observed particle morphology consisted of one or several nano-silica particles observed at random with a magnification of 100 times and 5000 times. The 100 times magnification was used to observe the particle size distribution, while the 5000 times magnification used to observe single-particle morphology. The observed particle size distribution was not uniform; specifically, the PDI values that were higher than 0.1 indicated that the homogeneity size was not too uniform. Through single-particle morphology, it could be seen that the nano-silica particles had flakes and a polygonal shape. Moreover, it could be seen that a single particle was comprised of several parts of crystals. In addition, the precipitation method produced nano-silica with polygonal morphology. Figure 4 shows the particle morphology of the nano-silica.

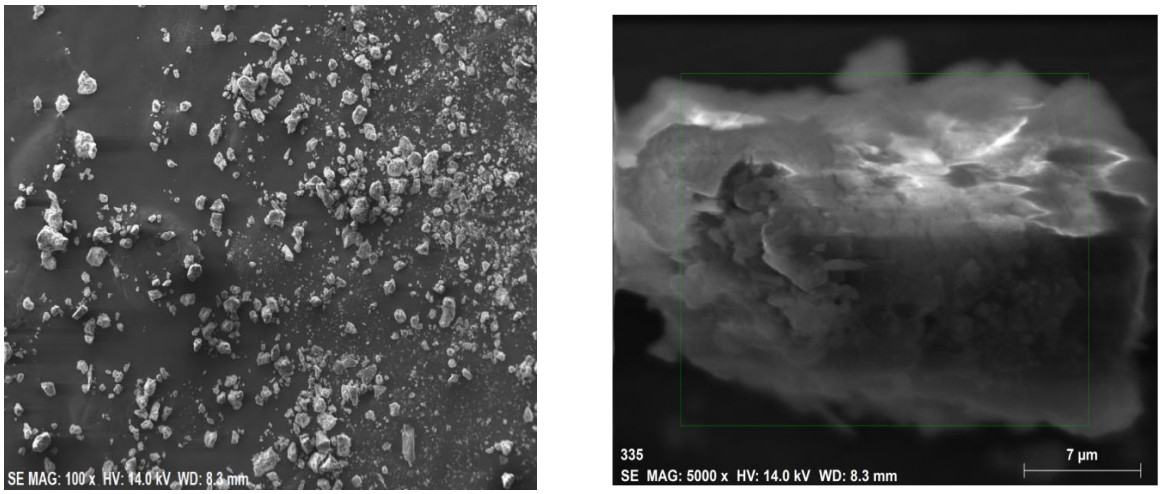

(a) (b)

Figure 4 Particle morphology of the nano-silica at: (a) 100×; and (b) 5000×

EDX and mapping observations showed that the nano-silica particle was primarily composed of Si and O. Beside Si and O, there were also elements of C and Na. The carbon (C) element may have resulted from the use of a sample preparation plate made from carbon. The Na element resulted from salt Na_2SO_4 (by-products from the production of silica) that was still attached to the nano-silica particle. Overall, the Si element had a percentage of 18.95% (wt), and the O element had a percentage of 25.31% (wt). Table 3 shows the elements of the particle based on an EDX test at 5000 times magnification.

Table 3 The elements of the nano-silica particle based on the EDX test

Element	Net Weight (wt %)	Atomic (wt %)
O	25.31	42.37
Si	18.95	18.07
C	14.48	32.30
Na	5.13	5.98
Pb	4.43	0.57
Cl	0.95	0.72
Total	69.26	100.00

3.3. The Potential Applications of Nano-silica

Nano-silica can be applied as a filler of composite materials. Nano-silica can improve the mechanical properties and durability of high-performance concrete of composite materials (Eddhie, 2017). Variations of the precipitation pH and the aging time influence nano-silica characterization and properties, which should be analyzed for appropriate potential applications. Table 4 shows the potential applications of nano-silica based on research and literature studies.

Table 4 Potential applications of nano-silica based on its characteristics

Combination	Characteristics of nano-silica			Potential application
	Degree of crystallinity (%)	Crystal size (nm)	Particle size (nm)	
pH 7 with 3 h of aging time	66.387	37.772	214.04	Direct methanol fuel cell (DMFC) membrane and supplementary cementitious material (SCM) need a composite with hydrophilic properties (low degree of crystallinity), particle size in nano order, and PDI < 0.7
pH 7 with 6 h of aging time	82.377	45.651	331.95	Additional support layer membrane ultrafiltration and composite resin need a semi-crystalline composite, particle size in nano order, and PDI < 0.7
pH 8 with 3 h of aging time	83.275	43.993	243.69	
pH 8 with 6 h of aging time	86.076	51.856	338.69	Rubber airbags need a composite with high crystallinity, particle size in nano order, and PDI < 0.7
pH 9 with 3 h of aging time	86.503	47.024	345.89	
pH 9 with 6 h of aging time	92.794	53.849	411.05	

3.3.1. Electrolyte membrane direct methanol fuel cell (DMFC) filler

The electrolyte membrane is the key component of the direct methanol fuel cell (DMFC), which transfers protons from an anode to a cathode. Using inorganic material as a membrane filler would increase proton conductivity due to its good hydrophilic properties (Setiawan et al., 2015). A decrease in the degree of crystallinity would increase the hydrophilicity properties (Yudhistira et al., 2012). In the present study, it was evident that pH 7 and an aging time of three hours produced the lowest degree of crystallinity. The high hydrophilic group of composites would improve the transfer of protons in the membrane electrolyte. Therefore, nano-silica is appropriate to be used as a composite electrolyte membrane due to the increase in the surface area.

Nano-silica can be applied to any polymer, such as chitosan, polysulfone, or polyetheretherketone. Ismayana et al. (2018) applied nano-silica from the boiler ash of the sugar cane industry as a filler of polysulfone (PSF) and sulfonated polyetheretherketone (sPEEK) membranes in DMFC. A membrane with a PSF:sPEEK ratio of 1:12 and the addition of 3% of nano-silica was the best composition with water absorption, methanol absorption, ion exchange capacity, and ionic conductivity values of 27.21%, 25.62%, 2.56 meq/g, and 66.28×10^{-6} S/cm, respectively (Ismayana et al., 2018). Indrasti et al. (2018) applied nano-silica as a filler of chitosan sulfate membranes in DMFC. A membrane with 0.1 M of ammonium sulfate and 3% of nano-silica had the highest performance with 40.75% of water absorption, 44.22% of methanol absorption, 0.66 meq/g of ion exchange capacity, and 6.48×10^{-4} S/cm of ion conductivity (Indrasti et al., 2018).

3.3.2. Additional support layer ultrafiltration membrane filler

Membrane technology is a new waste treatment method that improves the quality of the effluent (Faisal et al., 2016). An ultrafiltration membrane could replace chemical wastewater treatment with a lower cost and lower chemical use. The most common membrane used is a polysulfone membrane because it has good mechanical, thermal, and chemical stability. As a hydrophobic membrane, nano-silica needs to be used as a composite to increase the hydrophilicity of the polysulfone membrane so that the absorption is more effective. Windiastuti et al. (2016) showed that a polysulfone membrane with an addition of 3% of nano-silica could reduce the chemical oxygen demand (COD) by up to 8 mg/L, decrease the microbial content, and reduce the heavy metal content.

According to Yudhistira et al. (2012), an ultrafiltration membrane needs a lower hydrophilic composite and a larger particle size than the composite of a thin surface layer to support high flux. The combination of pH 7 and an aging time of six hours and the combination of pH 8 and an aging time of three hours resulted in nano-silica with the characteristics and properties that were appropriate for the support layer of an ultrafiltration membrane.

3.3.3. Composite resin filler

A composite resin is used in dentistry to restore cavities. The reaction of nanoparticles with composite resin would improve properties, such as wear resistance, smooth surfaces, elasticity, flexural strength, and tensile strength (Atai et al., 2012). Meanwhile, the addition of nano-sized filler material would result in increased surface area and water absorption. Therefore, the addition of nano-silica with a semi-crystalline degree of $45\% < x < 85\%$ is required. Nano-silica classified as semi-crystalline would have the number of siloxane groups higher than the silanol groups. Siloxane groups would prevent the absorption of excess water in the resin composite. The combination of pH 7 and an aging time of six hours and the combination of pH 8 and an aging time of three hours resulted in nano-silica that was fit for application as a composite resin filler.

3.3.4. Ship rubber airbag filler

A rubber airbag is a rubber product used for launching ships from the shipyard (Siswanto et al., 2012). Silica in a crystalline form would have more process capability than silica in an amorf form. Nano-silica would increase the surface area, making it more interactive with the rubber compounds. Nano-silica produced from a combination of pH 10 and aging times of three or six hours had a high degree of crystallinity.

3.3.5. Supplementary cementitious material (SCM) for concrete

Silica can be utilized as supplementary cementitious material because it can fill empty pores due to hydration of the cement paste as it is 100 times smaller than cement (Quercia and Brouwers, 2010). Through this mechanism, the density of the cement paste would increase. Based on SCM application needs, nano-silica with high reactive groups could support the bond between the silica and the cement. Silanol is a group of reactive silica that could increase the bond between the cement and the nano-silica. The combination of pH 7 and an aging time of three hours produced nano-silica with the lowest degree of crystallinity or domination by silanol groups.

4. Conclusions

The precipitation method produced nano-silica with polygonal morphology. Precipitation pH and aging time affected the characteristics of the nano-silica, including the particle size, PDI, crystal size, crystallinity degree, and crystal phase. The combination of various precipitation pH and aging times resulted in nano-silica with different characteristics. Overall, the nano-silica in this research had a semi-crystalline

to crystalline form with three crystal phases: tridymite, quartz, and cristobalite. Nano-silica has several potential applications, namely, as filler for DMFC membranes, ultrafiltration membranes, rubber airbag launchers, composite resin, and SCM.

Acknowledgements

This research was supported by the General Directorate of Strengthening Research and Development of the Ministry of Research, Technology, and Higher Education of the Republic of Indonesia through the Grant of Competence (*Hibah Kompetensi*) Scheme (Grant Number: 011/SP2H/LT/IV/2017 and Contract Addendum: 011/SP2H/LT/DRPM/VIII/2017).

References

Adam, F., Thiam-Seng, C., Andas, J., 2011. A Simple Template-free Sol Gel Synthesis of Spherical Nano-silica from Agricultural Biomass. *Journal of Sol-Gel Science Technology,* Volume 59(3), pp. 580–583

Allaedini, G., Muhammad, A., 2013. Study of Influential Factors in the Synthesis and Characterization of Cobalt Oxide Nanoparticles. *Journal of Nanostructure in Chemistry,* Volume 3, pp. 77–94

Arif, E., Clark, M.W., Lake, N., 2017. Sugar Cane Bagasse Ash from a High-efficiency Co-generation Boiler as Filler in Concrete. *Construction and Building Materials,* Volume 151, pp. 692–703

Atai, M., Pahlavan, A., Moin, M., 2012. Nano-porous Thermally Sintered Nano Silica as Novel Fillers for Dental Composites. *Dental Materials*, Volume 28(2), pp. 133–145

Bauccio, M., 1993. *ASM Metals Reference Book Third Edition*. ASM International, United States of America

Dhaneswara, D., Fatriansyah, J.F., Situmorang, F.W., Haqoh, A.N., 2020. Synthesis of Amorphous Silica from Rice Husk Ash: Comparing HCl and CH_3COOH Acidification Methods and Various Alkaline Concentrations. *International Journal of Technology,* Volume 11(1), pp. 200–208

Dileep, P., Narayanankutty, S.K., 2020. A Novel Method for Preparation of Nano-silica from Bamboo Leaves and its Green Modification as a Multi-functional Additive in Styrene-butadiene Rubber. *Materials Today Communications,* Volume 24, pp. 1–40

Eddhie, J., 2017. Strength Development of High-performance Concrete using Nano-silica. *International Journal of Technology*, Volume 8(4), pp. 728–736

Faisal, M., Machar, I., Gani, A., Daimon, H., 2016. The Combination of Air Flotation and a Membrane Bioreactor for the Treatment of Palm Oil Mill Effluent. *International Journal of Technology*, Volume 7(5), pp. 767–777

Ha, S.W., Weiss, D., Weitzmann, M.N., Beck, G.R., 2019. *Applications of Silica-based Nanomaterials in Dental and Skeletal Biology.* Nanobiomaterials in Clinical Density Second Edition, pp. 77–112, Lincoln, United Kingdom

Happy, Tok, A.I.Y., Su, L.T., Boey, F.Y.C., Ng, S.G., 2007. Homogeneous Precipitation of Dy_2O_3 Nanoparticles—Effects of Synthesis Parameters. *Journal of Nanoscience and Nanotechnology,* Volume 7(3), pp. 1–9

Indrasti, N.S., Ismayana, A., Damayanti, R., Maddu, A., Aryanto, A.Y., 2018. Utilization of Nanosilica from Boiler Ash Sugar Cane Industry for Filler of Chitosan Sulfate Membrane on Direct Methanol Fuel Cell. *In:* IOP Conferece Series: Earth and Environmental Science*,* Volume 196, pp. 1–6

Ismayana, A., Maddu, A., Sailah, I., Mafquh, E., Indrasti, N.S., 2017. Synthesis of Nano-silica from Boiler Ash of Sugar Cane Industry with Ulrasonication Method and Addition of Surfactant. *Journal of Agroindustrial Technology*, Volume 27(2), pp. 228–234

Ismayana, A., Maddu, A., Istifani, Y., Indrasti, N.S., 2018. Nanosilica from the Boiler Ash of the Sugar Cane Industry as a Filler of Polysulfone and Sulfonated Polyetheretherketone Membranes in Direct Methanol Fuel Cell. *Journal of Agroindustrial Technology*, Volume 28(1), pp. 104–112

Jalilpour, M., Fathalilou, M., 2012. Effect of Aging Time and Calcination Temperature on the Cerium Oxide Nanoparticles Synthesis via Reverse Co-precipitation Method. *International Journal of the Physical Sciences*, Volume 7(6), pp. 944–948

Jarvenin, G., 2013. *Precipitation and Crystallization Processes.* Los Alamos National Laboratory, Los Alamos, New Mexico

Lee, Y.R., Soe, J.T., Zhang, S., Ahn, J.W., Park, M.B., Ahn, W.S., 2017. Synthesis of Nanoporous Materials via Recycling Coal Fly Ash and Other Solid Wastes: A Mini Review. *Chemical Engineering Journal,* Volume 317, pp. 821-843

Mahdavi, M., Ahmad, M.B., Haron, M.J., Namvar, F., Nadi, B., Rahman, M.Z.A., Amin, J., 2013. Synthesis, Surface Modification and Characterization of Biocompatible Magnetic Iron Oxide Nanoparticles for Biomedical Applications. *Molecules*, Volume 18(7), pp. 7533–7548

Munasir., Surahmat, H., Triwikantoro., Zainuri, M., Darminto., 2013. Pengaruh Molaritas NaOH pada Sintesis Nanosilika Berbasis Pasir Bancar Tuban (*Effect of NaOH Molarity on Synthesis of Nano-silica from Tuban Bancar Sand*). *Jurnal Penelitian Fisika dan Aplikasinya,* Volume 3(2), pp. 12–17 (in Bahasa)

Namazi, H., Fathi, F., Heydari, A., 2012. *Nanoparticles based on Modified Polysaccharides*. Intech, Iran

Nidhin, M., Indumathy, R., Sreeram, K., Nair, B.U., 2008. Synthesis of Iron Oxide Nanoparticles of Narrow Size Distribution on Polysaccharide Templates. *Bulletin Material Sciences,* Volume 31(1), pp. 93–96

Okoronkwo, E.A., Imoisili, P.E., Olusunle, S.O.O., 2013. Extraction and Characterization of Amorphous Silica from Corn Cob Ash by Sol-gel Method. *Chemistry and Materials Research,* Volume 3(4), pp. 68–72

Quercia, G., Brouwers, H.J.H., 2010. Application of Nano-silica (nSi) in Concrete Mixtures. *In:* 8th fib PhD Symposium in Civil Engineering, At Lyngby, Denmark

Setiawan, W.K., Indrasti, N.S., Suprihatin., 2015. Synthesis and Characterization of Nano-silica from Boiler Ash with Co-precipitation Method. *In:* Proceeding International Conference of Adaptive and Intelligent Agroindustry (ICAIA), pp. 160–164

Shahmiri, M., Ibrahim, N.A., Zainuddin, N., Asim, N.B., Bakhtyar, B., Zaharim, A., Sopian, K., 2013. Effect of pH on the Synthesis of CuO Nanosheets by Quick Precipitation Method. *WSEAS Transactions on Environment and Development*, Volume 9(2), pp. 137–145

Singh, N., Dhruvashi, Kaur, D., Mehra, R.M., Kapoor, A., 2012. Effect of Aging in Structural Properties of ZnO Nanoparticles with pH Variation for Application in Solar Cells. *The Open Renewable Energy Journal*, Volume 5(1), pp. 15–18

Siswanto, Hamzah, M., Mahendra, A., Fausiah., 2012. Nano-silica Engineering Made from Local Silica as Filler of Compound Rubber Air Bag Ship Launcher from Shipyard. *In:* Proceeding Incentives of National Innovation System Research (INSINAS), pp. 56–59

Sriyanti, S., Taslimah, T., Nuryono, N., Narsito, N., 2005. Pengaruh Keasaman Medium dan Imobilisasi Gugus Organik pada Karakter Silika Gel dari Abu Sekam Padi (*The Effect of Medium Acidity and Organic Group Immobilized for Characters of Silica Gel from Rice Hull Ash*). *J. Kim. Sains & Apl.,* Volume 8(3), pp. 74–80 (in Bahasa)

Thuadaij, N., Nuntiya, A., 2008. Preparation of Nano-silica Powder from Rice Husk Ash by Precipitation Method. *Chiang Mai Journal Sciences,* Volume 35(1), pp. 206–211

Windiastuti, E., Suprihatin, Indrasti, N.S., 2016. Effectiveness of Polisulfon Membrane with Nano-silica Addition of Boiler Ash of Sugar Industry. *In:* Proceeding of the USR International Seminar of Food Security (UISFS), pp. 195–203

Yadav, V.K., Suriyaprabha, R., Khan, S.H., Singh, B., Gnanamoorthy, G., Choudhary, N., Yadav, A.K., Kalasariya, H., 2020. A Novel and Efficient Method for the Synthesis of Amorphous Nano-Silica from Fly Ash Tiles. *Materials Today: Proceedings*. pp. 1–5

Yudhistira, A.D., Iswanto, F.B., Kusworo, T.D., 2012. Preparation of Asymmetric Membrane for Water Treatment: The Effect of Evaporation Rime on Membrane Performance. *Journal of Chemical Technology and Industry,* Volume 1(1), pp. 186–193